ChemComm

FEATURE ARTICLE

View Article Online
View Journal | View Issue

Cite this: *Chem. Commun.*, 2023, **59**, 14776

From construction to application of a new generation of interlocked molecules composed of heteroditopic wheels

Mandira Nandi,†‡ Somnath Bej,†§ Tarun Jana and Pradyut Ghosh *

Received 4th August 2023,
Accepted 15th November 2023

DOI: 10.1039/d3cc03778a

rsc.li/chemcomm

Over the last few decades, research on mechanically interlocked molecules has significantly evolved owing to their unique structural features and interesting properties. A substantial percentage of the reported works have focused on the synthetic strategies, leading to the preparation of functional MIMs for their applications in the chemical, materials, and biomedical sciences. Importantly, various macrocyclic wheels with specific heteroditopicity (including phenanthroline, amide, amine, oxy-ether, isophthalamide, calixarene and triazole) and threading axles (bipyridine, phenanthroline, pyridinium, triazolium, *etc.*) have been designed to synthesize targeted multifunctional mononuclear/multinuclear pseudorotaxanes, rotaxanes and catenanes. The structural uniqueness of these interlocked systems is advantageous owing to the presence of mechanical bonds with specific three-dimensional cavities. Furthermore, their multi-functionalities and preorganised structural entities exhibit a high potential for versatile applications, like switching, shuttling, dynamic properties, recognition and sensing. In this feature article, we describe some of the most recent advances in the construction and chemical behaviour of a new generation of interlocked molecules, primarily focusing on heteroditopic wheels and their applications in different directions of the modern research area. Furthermore, we outline the future prospects and significant perspectives of the new generation heteroditopic wheel based interlocked molecules in different emerging areas of science.

School of Chemical Sciences, Indian Association for the Cultivation of Science, Kolkata 700032, India. E-mail: icpg@iacs.res.in
† M. Nandi and S. Bej contributed equally.
‡ Present Address: Organic & Medicinal Chemistry, CSIR-Indian Institute of Chemical Biology.
§ Present Address: Department of Chemical Sciences, Indian Institute of Science Education and Research Kolkata.

1. Introduction

Since the creation of mechanically interlocked molecules (MIMs), synthetic methods for the construction of multi-functional MIMs have become significantly important and

Mandira Nandi

Dr. Mandira Nandi received her BSc degree in 2012 from Asutosh College at the University of Calcutta in India. She earned her Master's degree in 2014 from IIT (ISM) Dhanbad, India and was awarded gold medal for being the topper. In 2020, she has been awarded PhD in Chemistry under the supervision of Prof. Pradyut Ghosh in IACS Kolkata, India. Currently, she is working as post-doctoral research associate at IICB, Kolkata, Kolkata. Her PhD research work covered the development of heteroditopic wheel-based mechanically interlocked molecules (MIMs) such as pseudorotaxanes, rotaxanes and catenanes and their applications.

Somnath Bej

Dr. Somnath Bej graduated from Ramakrishna Mission Vivekananda Centenary College, Rahara, India in 2012. He graduated with a Master's in Chemical Sciences in 2014 from Indian Institute of Technology Kharagpur (IIT Kharagpur) in India. He received his PhD in Chemistry in 2020 from IACS Kolkata, India, under the direction of Prof. Pradyut Ghosh. Currently, he is working as a post-doctoral research associate at IISER Kolkata. His PhD research work included designing of fluorophoric/chromophoric heteroditopic wheel-based pseudorotaxanes and rotaxanes.

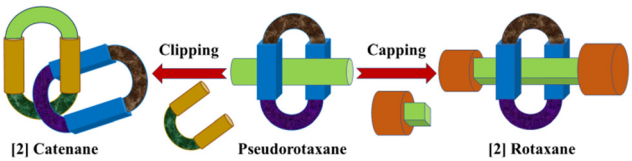

Scheme 1 An illustration of heteroditopic wheel based pseudorotaxane, rotaxane and catenane.

widespread because of their implementations in chemical, biological and materials sciences.[1] It is important to mention that a considerable amount of outstanding, significant works on MIMs and their numerous applications[1,2] earned the Nobel Prize in Chemistry in 2016. MIMs with essential mobile components, which are held together by non-covalent interactions, are classified into two main interlocked architectures: rotaxanes and catenanes. In both cases, pseudorotaxanes act as primary building blocks (Scheme 1). The synthesis and applications of such threaded/interlocked molecules mainly depend on the logical designing of their main constituent components, *i.e.*, wheel (host) and axle (guest). The strategic incorporation of various functional groups in the wheel and axle components enhances the host–guest interactions through metal coordination, hydrogen/halogen bonding, π–π stacking, and other interactions for the development of various newer multifunctional MIMs.[2] In recent years, by incorporating cation/anion templating, photo/redox-active, and π–π stacked moieties, a series of different macrocyclic/bicyclic wheels and numerous corresponding axles have been introduced.[3] Moreover, varieties of supramolecular systems have been popularized for the construction of novel threaded molecules for broader applicability in sensing, switching/shuttling, drug delivery agents, bio-imaging, catalysis and other areas. A literature survey shows that few reviews have emphasized the wheels specifically made of pillar-arene,[4] cyclodextrin,[5] calixarene,[6] crown ether,[7] cucurbituril[8] and other molecules for the synthesis of MIMs.[9] A recent article by Evan's group reviewed heteroditopic rotaxanes and catenanes for ion-pair recognition.[10] However, a detailed discussion on new generation heteroditopic macrocycle/bicycle directed MIMs along with their significance in different directions has not yet been presented. In this feature article, we present up-to-date (2023) design aspects for the application of new-generation interlocked molecules, mainly focusing on heteroditopic wheels. Our objective is to provide a comprehensive overview that describes the latest developments, synthetic methods and significant applications of pseudorotaxanes, rotaxanes and catenanes composed of heteroditopic wheels with suitable threading components.

2. Macrocyclic wheels with heteroditopicity

Macrocyclic wheels composed of different functionalities offer higher binding affinities with the guest axle *via* various non-covalent interactions. In this regard, as compared to monotopic wheels, the designing of heteroditopic macrocycles/bicycles might be of greater interest, as it essentially consists of different functionalities or groups to generate heteroditopicity in the wheel. Depending on the different embedded functionalities, heteroditopic wheels can provide donor–acceptor interactions, metal–ligand coordination, π–π stacking, hydrogen bonding, hydrophobic interactions, *etc.*, towards the construction of new

Tarun Jana

Tarun Jana graduated from Vidyasagar University, India in 2019. In 2021, he obtained his Master's degree from Banaras Hindu University, Varanasi, India in Chemistry. Currently, he started his research career under the guidance of Prof. Pradyut Ghosh at IACS Kolkata, India. He is working on the development of new heteroditopic wheels and new generation mechanically interlocked molecules (MIMs) along with their machinery properties.

Pradyut Ghosh

Prof. Pradyut Ghosh is a senior professor in the School of Chemical Sciences at the Indian Association for the Cultivation of Science (IACS), India. He received his PhD in Chemistry from the Indian Institute of Technology, Kanpur under the direction of Parimal K. Bharadwaj in 1998. He spent two years as a post-doctoral fellow at Texas A&M University, with Richard M. Crooks and he was an Alexander von Humboldt Fellow at the University of Bonn, Germany in Fritz Vögtle's and Christoph A. Schalley group. Upon his return to India, he joined Central Salt & Marine Chemicals Research Institute, India and in 2007 he moved to IACS. His present research interests are covering the designing of Interlocked Molecular Systems, Recognition, Sensing and Extraction of ion and Ion-pair, Supramolecular and Photo Catalysis.

generation novel MIMs[11] to serve in switching, shuttling, sensing, ion pair recognition, *etc.*[12]

Herein, we present some of the most representative heteroditopic wheels containing different suitable functionalities, including phenanthroline (phen), oxy-ether, amide, amine, triazole, *etc.* (Fig. 1). In this direction, Sauvage and co-workers reported a phen/terpyridine-oxy-ether containing heteroditopic macrocycle (**W1**) and several MIMs *via* the metal templation technique (Fig. 1).[13] To explore metal templation based multifunctional MIMs further, Ghosh and co-workers recently developed several new combinations of heteroditopic macrocycles, *i.e.* amido-triamine (**W2**),[14] oxy-ether-triamine (**W3**, **W4**)[15] and oxy ether-Phen-ester (**W5**)[16] wheels. Using anion templation, Beer and co-workers developed different heteroditopic macrocycles depending on isophthalamide/calix[4]diquinone/triazole/oxy-ether (**W6–W7**, **W9**) motifs.[17] Within such wheels, the threading of the pyridinium axle component leads to anion templation. Afterwards, the modification of the pyridinium axle with pyridine-*N*-oxide and 4-iodopyridyl-2,6-dicarbonyl moieties is directed towards the metal temptation approaches. Another type of imine oxy-ether heteroditopic wheel (**W8**) was recently reported by the Chiu group and utilised in alkali metal templated MIMs.[18] In 2000, the first synthesis of an isophthalamide-crown ether-based heteroditopic macrobicycle was reported by Smith's group (**W10**).[19] Later, an amido-amine functionalized heteroditopic macrobicyclic host (**W11**)[20] with two distinct cavities to be utilized in the recognition of different guests through hydrogen bonding interaction was reported by our group. Other significant functionalities like naphthyl, phenyl, naphthalene tetracarboxylic di-imide (NDI), paraquat, *etc.*, have also been incorporated within the wheel and/or in the axles to introduce multifunctional properties within the MIMs. Moreover, besides these wheels (Fig. 1), other relevant heteroditopic macrocycles/bicycles associated with important MIMs are also discussed in later sections.

3. Mechanically interlocked architectures with heteroditopic wheels

The design and synthesis of threaded/interlocked molecules composed of multiple functionalities and suitable groups are one of the current research topics on interlocked systems. Historically, the first catenane and rotaxane were invented by Frisch-Wasserman[21] and Harrison and coworkers,[22] respectively. Further, Sauvage *et al.* introduced the phen-ether (**W1**) heteroditopic wheel for the synthesis of Cu^{I} templated [2]catenanes with high yield.[23] Leigh and co-workers introduced a conceptually novel active metal templation approach in which the reactive unit is mainly the macrocycle-metal ion complex that helps to organise the wheel-axle components and facilitates the formation of MIMs.[2a] Beyond these active and passive metal templation approaches, several noncovalent interactions, including hydrogen/halogen bonding (HB/XB), π–π stacking interaction, anion templation, *etc.*, have also been introduced between the wheel and axle for the synthesis of high yielding MIMs.[24] In the designing of such MIMs (pseudorotaxanes, rotaxanes or catenanes) by different templation approaches, heteroditopic macrocyclic/bicyclic wheels play an important role, as heteroditopicity brings versatility within the MIM systems. Therefore, in this section, we will explain in detail the latest works related to the construction of the above discussed heteroditopic wheel-based multifunctional pseudorotaxanes, rotaxanes and catenanes.

3.1. [*n*]Pseudorotaxanes (*n* = 2, 3, 4)

Pseudorotaxanes are the fundamental unit for the synthesis of rotaxanes and catenanes through the capping and clipping approaches (Scheme 1). In the literature to date, several [*n*]pseudorotaxanes have been reported with some conventional

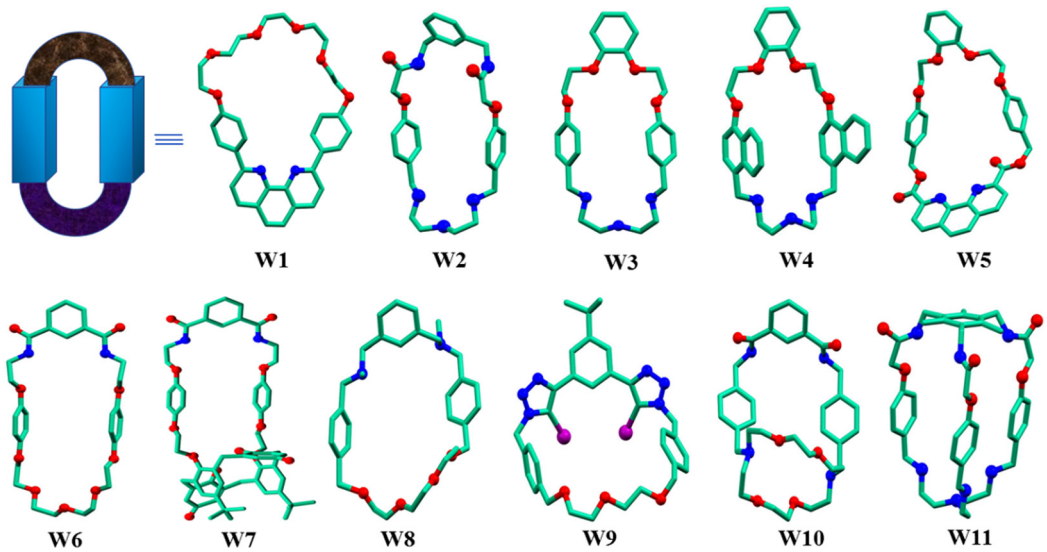

Fig. 1 Representative heteroditopic wheels with different functionalities (atoms are represented by blue for N, red for O and violet for I).

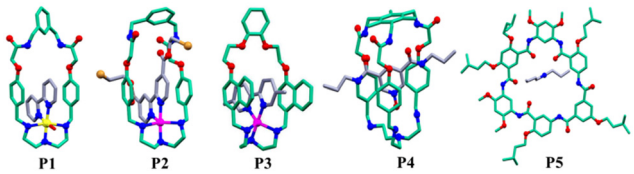

Fig. 2 The representative crystal structures of [2]pseudorotaxanes. (Data from the Cambridge Crystallographic Data Centre, (CCDC); **P1**: 839502, **P2**: 1534187, **P3**: 1589356, **P4**: 1063853, and **P5**: 976751. Atoms are represented by blue for N, red for O, yellow for Ni and pink for Cu).

supramolecular wheels like crown ether, pillar arenes, cucurbiturils, *etc.*, towards the formation of MIMs. However, in this subsection, we will describe the [*n*]pseudorotaxanes utilizing different heteroditopic wheels that have been synthesized and studied systematically (Fig. 2). In this context, our group has recently reported several new generation [2]pseudorotaxanes composed of the above discussed heteroditopic wheels (**W2–W5**) and 4,4′/5,5′-bipyridine, phen/paraquat derivatized axles *via* Cu^{II}/Ni^{II} templation, hydrogen bonding and π–π stacking interactions wherever applicable. In addition, self-sorting studies have been performed from a mixture of different bidentate chelating ligands (derivatives of phen and bipyridine) and metal ions (Co^{II}, Cu^{II}, Ni^{II}, Zn^{II}) to bind with the corresponding macrocycle **W2** and **W3**, respectively. This study assists in finding the most favourable combination of macrocycle, selective metal and chelating ligand to form stable [2]pseudorotaxane.[14,15] Furthermore, the crystal structure analysis confirmed that during ternary pseudorotaxane formation, Ni^{II} and Cu^{II} prefer the corresponding hexa (**P1**) and penta (**P2**, **P3**) orthogonal coordinations, respectively. Such coordination around the metal is satisfied by the tris amine moiety of the wheel, bidentate axle and solvent molecule wherever applicable (Fig. 2).[15b,25] Moreover, our group has also demonstrated macrobicyclic, **W11** and pyridine *N*-oxide axle-based HB templated [2]pseudorotaxane (**P4**) formation where the changes of the pyridine *N*-oxide axle direction within the wheel were studied.[20] Recently Yuan and co-workers constructed a different type of [2]pseudorotaxane (**P5**) by incorporating a heteroditopic cyclo[6]aramide wheel that shows binding of dibutyl ammonium chloride *via* HB interactions.[26]

The development of higher-ordered heteroditopic threaded molecules such as [3]/[4]/[5] pseudorotaxanes (Fig. 3) with unique structural architectures is also challenging from the synthetic point of view. In 1999, Sauvage and co-workers described Cu^{I} complexed heteroditopic [3] (**P6**) and [5] pseudorotaxanes, which served for [3] and [5]rotaxane formation *via* threading of the bis-chelating ligand within a **W1** wheel.[24a] They have also studied octahedral metal coordinated [3]pseudorotaxane (**P7**) and rotaxane formation *via* insertion of two bipyridine strings into the 8,8′-diphenyl-3,3′-bi-isoquinoline heteroditopic wheel.[27] In addition, our group has reported the Cu^{II} templated two station derivatized axle ([2,2′-bis(2-pyridyl)bi-benzimidazole]) threaded heteroditopic **W2** based [3]pseudorotaxane (**P8**) formation in which fluorescence switching is triggered *via* the axle substitution mechanism.[28] Furthermore, our group has systematically designed heteroditopic **W4** directed multinuclear fluorophoric [3]pseudorotaxane (**P9**) and [4]pseudorotaxane (**P10**), utilizing bipodal and tripodal functional phen axle motifs through Cu^{II}/Ni^{II} templation and π–π staking interactions.[29]

3.2. Rotaxanes

Over the past few years, several types of MIMs have been extensively explored by various researchers, including Sauvage,[30] Stoddart,[1f,2b] Gibson,[31] Leigh,[32] Tian,[33] Beer,[34]

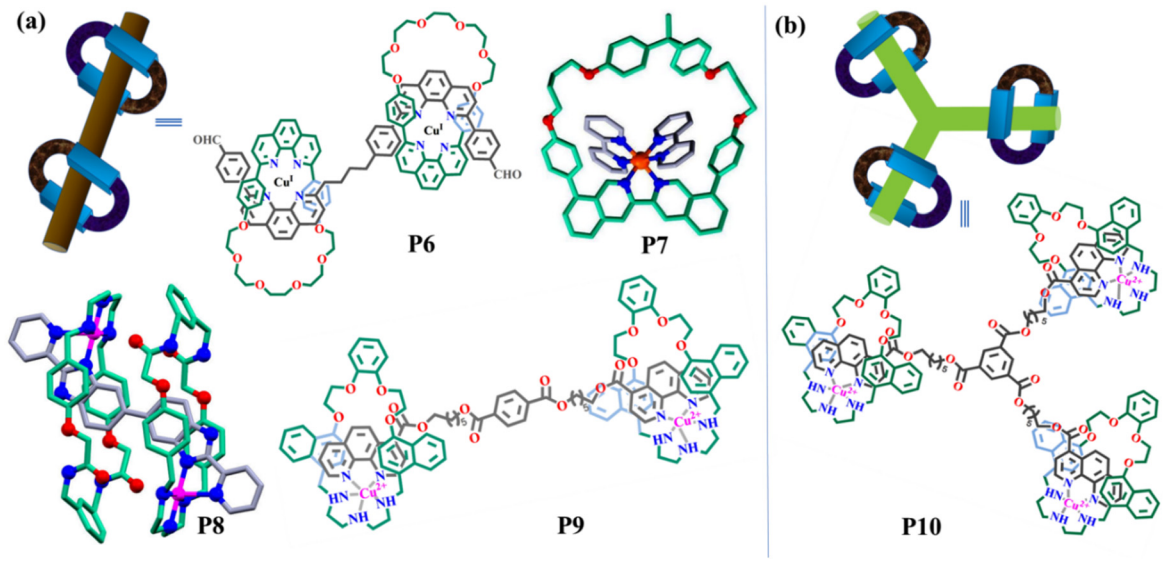

Fig. 3 Representative crystal and chemical structures of (a) [3]pseudorotaxanes (**P7** and **P8**, data from the Cambridge Crystallographic Data Centre (CCDC): **P7**: 736954, **P8**: 827910; atoms represented by blue for N, red for O, orange for Fe and pink for Cu) and (b) [4]pseudorotaxane. (Counter anions are omitted for clarity.)

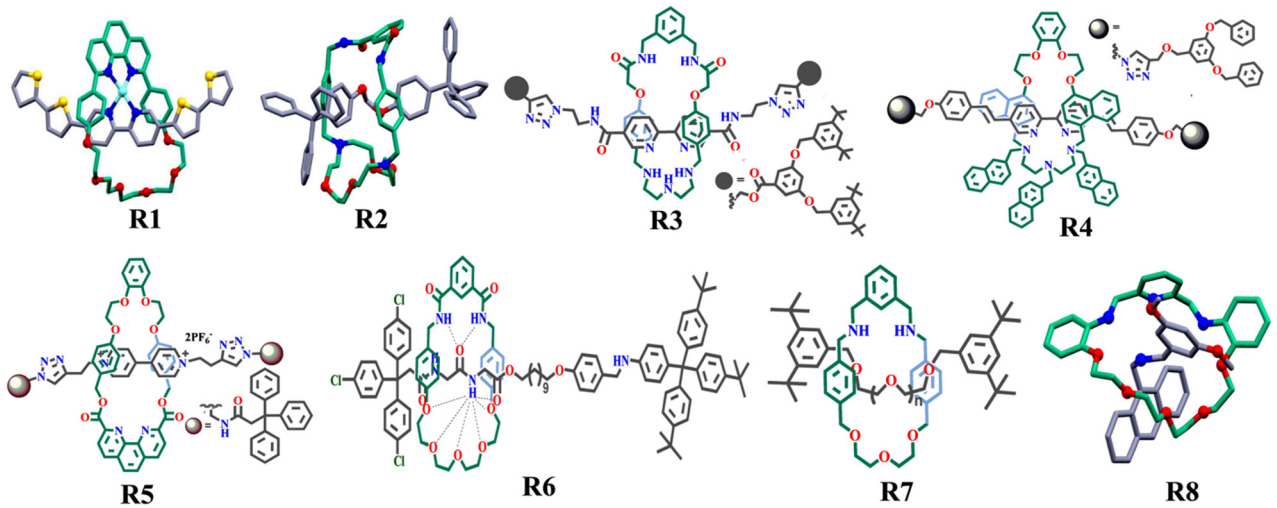

Fig. 4 The representative crystal and chemical structures of [2]rotaxanes (**R1**, **R2** and **R8**; data from the Cambridge Crystallographic Data Centre (CCDC): **R1**: 1277085, **R2**: 171663 and **R8**: 1942423. Atoms are represented by blue for N, red for O, yellow for S and sky blue for Zn.)

Smith,[35] Schalley,[36] Goldup,[37] Loeb,[38] Huang[39] and others.[40] In this subunit, several heteroditopic rotaxanes are described chronologically and the representative chemical structures of the rotaxanes are presented in Fig. 4. In 1996, conducting polymetallorotaxanes composed of the heteroditopic **W1** wheel and a thiophene connected bipyridine axle were reported by Swager and co-workers using Cu^{I}/Zn^{II} templation.[41] Likewise, based on the heteroditopic **W1** wheel and bi/tri dentate chelating axles (phen/terpyridine), Sauvage and co-workers reported several examples of Cu^{I} metallated heteroditopic [2]rotaxanes that were further utilised for switching, shuttling, *etc.*[42] In 2000, Smith and group reported a K^{I} bound heteroditopic [2]rotaxane (**R2**) composed of the **W10** macrobicycle and an acetal-containing axle moiety where the structural geometry of **R2** was confirmed by X-ray crystallography.[19,43] Subsequently, by following passive and active metal templation approaches, our group also demonstrated heteroditopic **W2–W5** wheel based multifunctional [2]rotaxanes (**R3–R4**, Fig. 4) by following CuAAC click chemistry for the sensing and recognition of ions.[25a,44] Similarly, a **W5** wheel based heteroditopic [2]rotaxane (**R5**) involving π–π stacking interaction was also reported by our group.[45] During such MIMs formation *via* passive/active metal ($Ni^{II}/Cu^{I/II}/Ca^{II}$) templation and π–π stacking interaction, several types of functionalized bipyridine, NDI and paraquat moiety containing axles have been thoughtfully utilised. Furthermore, some of the heteroditopic rotaxanes (**R12**, Fig. 9b and **R24**, Fig. 16a) were post functionalized by acyl/fluorophoric groups to fine tune the recognition and sensing properties.

Beyond the metal templation technique, Beer's group has recently reported various HB/XB heteroditopic [2]rotaxanes (**R6**, **R14**, Fig. 10 and **R26**, Fig. 17) directed by the **W6** and **W7** heteroditopic wheels for anion sensing and ion pair recognition. Additionally, they described the dynamicity of heteroditopic **W6** dependent higher ordered fluorophoric [3]rotaxanes (**R13** and **R14**, Fig. 10).[46] Likewise, with the heteroditopic **W6** wheel, both Leigh and Li's groups demonstrated HB templated heteroditopic [2]rotaxanes (**R10**, Fig. 7 and **R15**, Fig. 11b). In both cases, controlling the translation of the macrocycle from one station to another assists in molecular switching and shuttling.[17a,47] Leigh's group also synthesized the bifunctional pyridine-associated **W6** wheel, in which HB donor and acceptor moieties are present at different ends of the wheel. This eventually assists in stabilizing the axle-forming transition state that is developed during the formation of [2]rotaxane.[48]

In addition to these above mentioned rotaxanes, another type of heteroditopic [2]rotaxane (**R7**, Fig. 4 and **R17**, Fig. 12b) was described by Chiu's group utilising imino macrocycle (**W8**) in the threading of an oligo(ethylene glycol) motif axle by Na^{I} templation.[18,49] Leung's group reported a heteroditopic **W8** wheel based [2]rotaxane (**R8**) synthesized by the in-situ reaction of equimolar tetra-ethylene glycol bis(2-aminophenyl)ether, 2,6-pyridine dicarboxaldehyde and an anthracene/BODIPY-based axle *via* a clipping strategy.[50]

3.3. Catenanes

Since the revolutionary synthetic approach to designing a catenane by Sauvage and co-workers,[23,51] several methodologies have been developed to date. Here, heteroditopic wheel-based catenanes are discussed. The corresponding crystal structures and chemical diagrams are presented in Fig. 5. Significantly, Sauvage's group described Cu^{I} templated **W1** heteroditopic wheel and bidentate phenanthroline axle directed [2]catenanes (**C1**) and other higher ordered catenated systems.[51,52] During that same period, Stoddart and co-workers studied Cu^{I} complexed naphthyl and phen moiety embedded [2]catenane (**C2**) by incorporating a bis-paraquat motif in place of the oxy-ether of the **W1** wheel. The resulting [2]catenane undergoes circumrotation, where phen motifs from both the axle and wheel interact with the hydrogen ion upon addition of CF_3COOH.[53] In 2008, by utilising a **W1** type wheel,

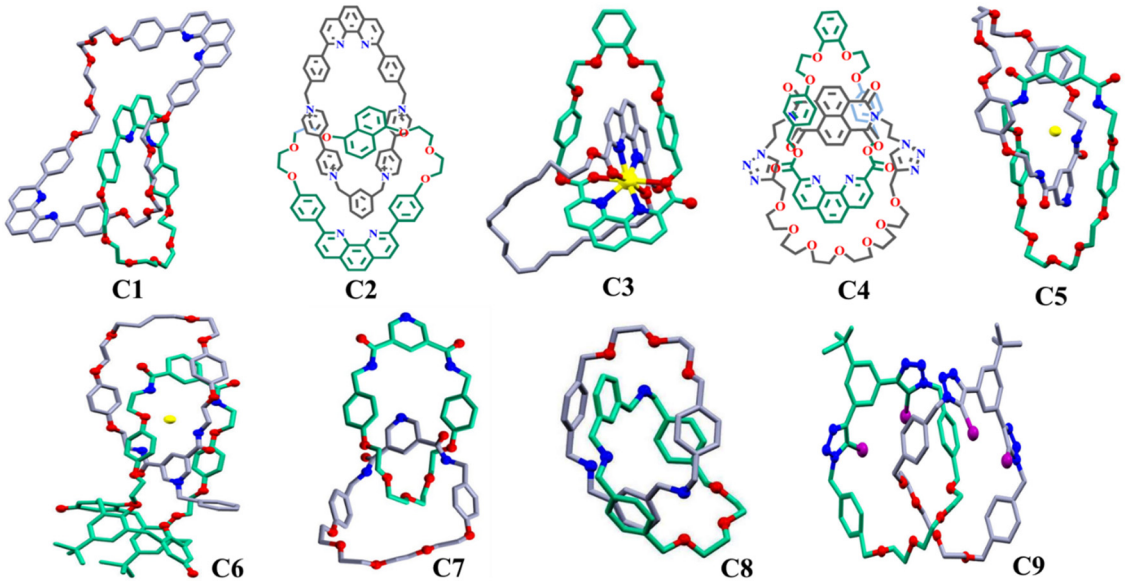

Fig. 5 The representative crystal and chemical structures of [2]catenanes (**C1**, **C3–C6**, **C8** and **C9**, data from the Cambridge Crystallographic Data Centre (CCDC): **C1**: 1254088, **C3**: 817352, **C4**: 809245, **C5**: 1889522, **C6**: 1871207, **C8**: 952636 and **C9**: 2211718. Atoms are represented by blue for N, red for O, yellow for Na and violet for I.)

Schuster and group demonstrated different mono/multinuclear heteroditopic catenanes.[54]

Correspondingly, our group demonstrated phen ester-oxy ether **W5** containing new multifunctional [2]catenanes (**C3** and **C4**) and the investigation of their use in cation and anion recognition/sensing.[16,55] In the case of Cu^{I} templated heteroditopic **C3**, the phen-ester moieties of both the axle and wheel counterparts are enabled to bind Na^{I} exclusively, that is, supported by the phen N and ester O atoms of wheel. Afterwards, the phen-ester moiety of **W5** and derivatized carbonyl moiety of the NDI axle assist in forming heteroditopic **C4** *via* Ca^{II} templation, by following a CuAAC reaction.[55]

Beer and co-workers described an anion templated heteroditopic **W6** wheel-dependent [2]catenane (**C5**) *via* the threading of the *N*-benzyl pyridinium amide cleft precursor into the wheel.[56] A similar approach is followed in the formation of the calix[4]diquinone-oxy ether (**W7**) based heteroditopic catenane **C6**, in which reversible rotary motion has been shown.[57] In addition, several HB and XB bonded heteroditopic catenanes based on **W6** and **W7** wheels have been reported by Beer's group.

Furthermore, Lewis and co-workers described the formation of a different type of heteroditopic homo [2]catenane (**C7**) *via* self-templation strategy by involving a pyridine unit containing two **W6** wheels, in which the pyridine metal nodes upon complexation with Ag^{I} yielded a coordination polymer.[58]

Recently, Na^{I} templated homo [2]catenanes (**C8** and **C9**) have been reported, with the heteroditopic **W8**[49a,59] and **W9**[17c] macrocycles, respectively, where the alkali metal prefers to bind in an orthogonal manner. By following a different approach, an amidinium carboxylate salt bridge-oxy ether directed heteroditopic optically active [2]catenane was also studied by Yashima and co-workers. In this case, an acid/base or Zn^{II} ion regulated the relative motion of the macrocyclic components.[60] Further, Gunnlaugsson and co-workers reported the self-assembly of bifunctional motifs, namely pyridine isophthalamide-oxy ether, to generate an Eu^{III} templated [3]catenane *via* RCM reaction.[61] These important embedded functionalities of heteroditopic MIMs have made them good candidates for utilization in various applications, such as recognition, sensing, switching, shuttling, catalysis, biological activities, *etc.*

4. Applications of heteroditopic interlocked molecules

In this section, we elaborate the applications of these new generation heteroditopic wheel-based multifunctional threaded/interlocked molecules. This part is divided into three sections according to the applications of the MIMs: (a) switching, (b) dynamic properties and (c) recognition-sensing.

4.1. Molecular switching of the threading systems

Threaded architectures, containing different types of functionalities, are potential systems for molecular switching which can be attained by various external stimuli, such as anions/cations, acid/base, heat, photoluminescence, solvent polarity, chemical reagents, *etc.* To date, numerous significant works have explored molecular switching, directed by differently functionalized MIMs. Herein, particularly, molecular switching will be discussed focusing on heteroditopic MIMs.

Pseudorotaxanes can easily show reversible threading/dethreading/rethreading processes upon tuning the binding capability of the axle functionality within the wheel component that leads to molecular switching and shuttling.[62] In this direction, an electrochemically driven double switching process

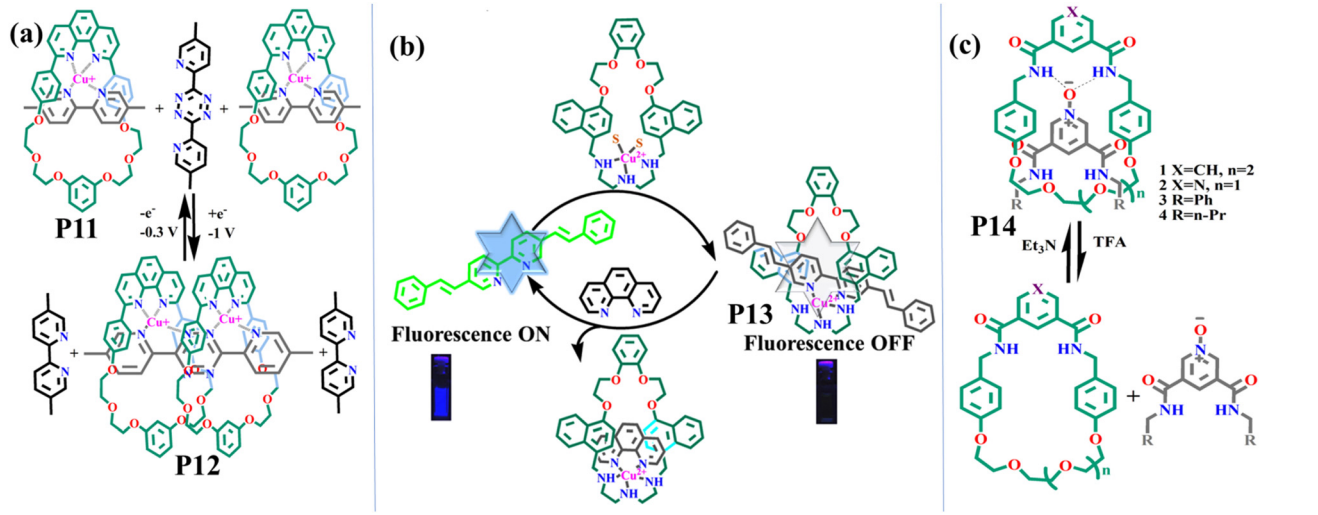

Fig. 6 (a) The electrochemical switching of **P11** and **P12**; (b) fluorescence switching of **P13** and (c) acid–base controlled switching of **P14**.

was described by Flood's group when utilizing a heteroditopic **W1** type wheel and bipyridine and tetrazine containing axles to design [2] and [3]pseudorotaxanes (**P11** and **P12**, Fig. 6a), respectively, *via* Cu^{I} templation. The kinetics of switching between these two corresponding axles within the macrocycle was examined by electrochemical analysis. They have also shown the reversible double switching of two wheels from two bipyridines to a reduced double-site tetrazine to produce a [3]pseudorotaxane (Fig. 6a).[63]

Our group reported fluorescence switching in the **W2** wheel-based heteroditopic non-fluorophoric pseudorotaxane **P8** (Fig. 3), where substitution of the bidentate fluorophoric axle (2,2′-bis(2-pyridyl)dibenzimidazole) with the stronger chelating phen motif causes a fluorescence 'ON' state.[28] A similar case of the fluorescence ON/OFF switching phenomenon was also studied in heteroditopic [2]pseudorotaxane **P13** (Fig. 6b), based on a **W4** wheel and fluorophoric bipyridine ligand derivative.

In this system, the fluorescence turned 'ON' upon the dethreading of the fluorescent bipyridine ligand *via* axle substitution with a stronger chelating phen ligand. Further, upon the rethreading of the bipyridine ligand, fluorescence is turned 'OFF' (Fig. 6b).[15b] In both cases, the axle substitution method and comparative binding studies were carried out by UV-Vis and fluorescence titration experiments. Furthermore, acid–base stimuli controlled dethreading/rethreading processes were demonstrated by Jiang and co-workers with [2]pseudorotaxane **P14** (Fig. 6c) by incorporating a pyridine *N*-oxide derivatized axle into a **W6** type heteroditopic amide-ether macrocycle (Fig. 6c).[64] In addition, heteroditopic pyridinyl **W8** wheel-dependent multilevel fluorescence switching in two stations (amide and amine) containing fluorophoric anthracene stoppered [2]rotaxane was reported by Li and co-workers (**R9**, Fig. 7a). Here, three successive independent movement processes of the wheel were shown. During the addition of acid, the wheel's ether part interacts with the axle amine station and trigger quenching of the anthracene fluorescence occurs due to the stronger photoinduced electron transfer (PET) process.

However, after the addition of base or Li^{I}, the fluorescence intensity is increased a bit, as the wheel shifts to the axle-amide station and PET is quenched due to the increment of spatial distance. After Zn^{II} addition, the wheel is shifted again on the axle-amine station to interact the wheel-amine counterpart with Zn^{II}; thus, the PET process is entirely OFF and the fluorescence intensity is recovered completely (Fig. 7a). All these processes were verified by NMR, UV-Vis and PL titration experiments.[65]

The Leigh group also developed multilevel molecular switching in heteroditopic [2]rotaxane (**R10**, Fig. 7b), featuring two stations (pyridinium and triazole) comprising the axle and a heteroditopic Pd templated pyridine adjoined **W8** wheel. The wheel, upon triggering with TBACl, switches to the axle-pyridinium station and thus the wheel-ether part is hydrogen bonded to the axle-pyridinium ion. Subsequently, upon anion extraction with the addition of $AgPF_6$, the Pd bound pyridine wheel reverts back to the axle-triazolium station to coordinate with the axle-triazolium moiety, which was established by comparative NMR experiments (Fig. 7b).[66]

Furthermore, Beer and group reported a neutral XB [2]rotaxane (**R11**, Fig. 8), composed of a heteroditopic amino triazole-oxy ether (**W9**) wheel and a halogen bonded amino-triazole based axle, which is able to show *ortho* steric-regulated switching controlled by the cation/anion guest moiety. Here, the Zn^{II} addition interacts with the amino-triazole core of both the wheel and axle components. However, in acidified **R11**, the axle-amine is protonated and H-bonded with the wheel-ether part and the counter anion (Cl^{-}) is halogen bonded to the iodine-triazolium core unit (Fig. 8).[67] Such heteroditopic mechanically interlocked molecular switches may further serve in molecular logic gates, responsive drug delivery, biological assays and nanotechnology.

4.2. Effect of mechanical bond in the dynamic properties

The incorporation of significant multi-functionalities into the rotaxanes and catenanes directs the innovative ideas of generating new dynamic properties with translational and

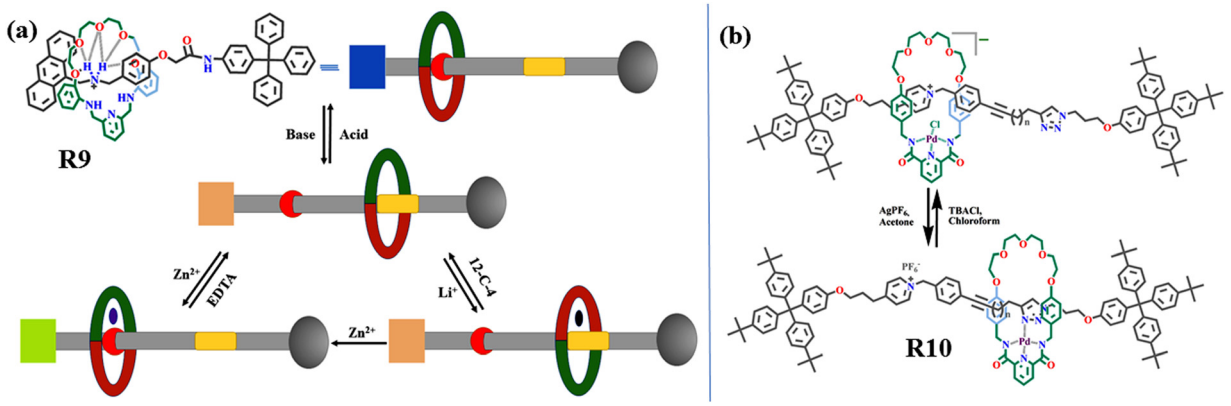

Fig. 7 (a) The acid/base/metal-controlled fluorescence switching of **R9**. (b) The anion-controlled switching of **R10**.

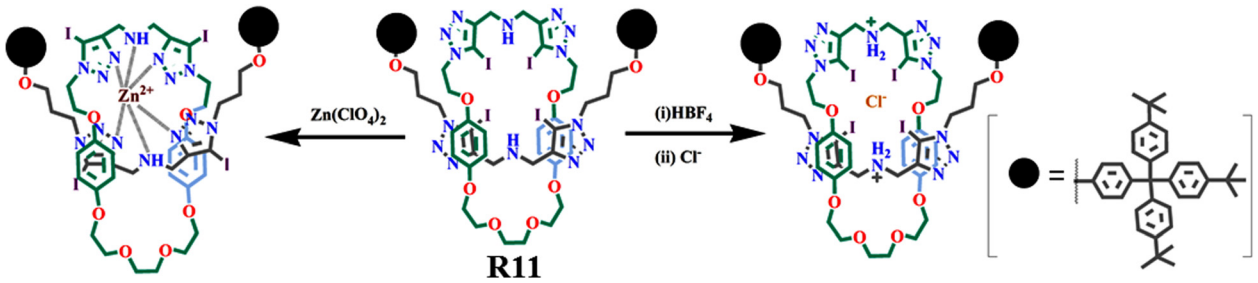

Fig. 8 The cation/anion regulated switching of **R11**.

rotational motions. Relative movement of non-covalently attached components produces reversible alternation or multiple controlling of the co-conformation of MIMs, *i.e.* can be triggered by external stimuli (cation/anion, acid/base) to fabricate smart molecular machineries, as reported by several groups.[68] In this subsection, we briefly summarize the effects of mechanical bonds on the dynamic properties of heteroditopic wheel-based MIMs.

In this context, Sauvage and co-workers reported **W1** dependent heteroditopic [2]catenane **C10**, in which mechanically bonded another wheel counterpart is phen–terpyridine, where rotation of one ring concerning the other is shown upon Cu^{I}/Cu^{II} coordination preferences (Fig. 9a).[30,69] Based on similar Cu^{I}/Cu^{II} binding modes, shuttling has also been studied in another heteroditopic [2]rotaxane by Sauvage and group.[42b] Significantly, in the case of this [2]rotaxane with respect to Cu^{I}/Zn^{II} metal binding, the chelating counterparts (phen and terpyridine) generate a ''molecular muscle'' which is lengthened or contracted on the basis of the interaction of wheel with the axle in response to external chemical stimuli.[42b,70] By following a different mechanism, our group also described dynamic properties within a tri-acetylated **W3** wheel based [2]rotaxane (**R12a**, Fig. 9b) system. It was shown that, upon subsequent addition and removal of alkali metal ions (Na^{I} and Li^{I}) in **R12a**, it exhibits reversible locking and unlocking of the dynamic behaviour, respectively, which was further verified with ^{1}H NMR experiments.[44b] Our group has also studied the structure–property relationship of another naphthalene substituted **W3** wheel based [2]rotaxane based on steric interaction *via* subsequent functionalization of the tri-amine moiety of the wheel with acetyl, aryl and *tert*-butyl groups. Variable temperature NMR analysis revealed that the tri-acylated and tri-aryl substituted rotaxanes showed diverse rotamer-induced conformations/co-conformations. However, *tert*-butyl substitution predominantly showed a single conformer due to the presence of the bulky *tert*-butyl group, which hindered tertiary amide bond rotations and displayed controlled dynamic behaviour.[71]

Beer's group designed two different heteroditopic **W6** wheel-based Cl^{-} templated [3]rotaxane hosts with two ferrocene and naphthalene adjoined motifs, of which only the naphthalene one is displayed (**R13**, Fig. 10a). Both the rotaxanes undergo a conformational change upon selective recognition of SO_4^{2-} to form a 1 : 1 ''sandwich'' complex, where SO_4^{2-} is linked between the bis-isophthalamide macrocyclic components in a closer proximity. Upon binding of SO_4^{2-}, abrupt fluorescence quenching of the naphthalene (**R13**) takes place and concurrent cathodic shifting is caused due to the ferrocene/ferrocenium redox couple.[46c,72] Anion-induced molecular shuttling was also described in another heteroditopic [3]rotaxane (**R14**, Fig. 10b) consisting of a central C_{60} fullerene and four stations (bis-triazolium and bis-NDI), including the axle and two ferrocenyl-functionalized **W6** wheels. ^{1}H NMR spectroscopy displayed that, upon addition of Cl^{-} or PF_6^{-} salt, the wheel moves to the axle-triazolium or NDI station. The positional change of the wheel to the axle stations was also examined by steady-state and

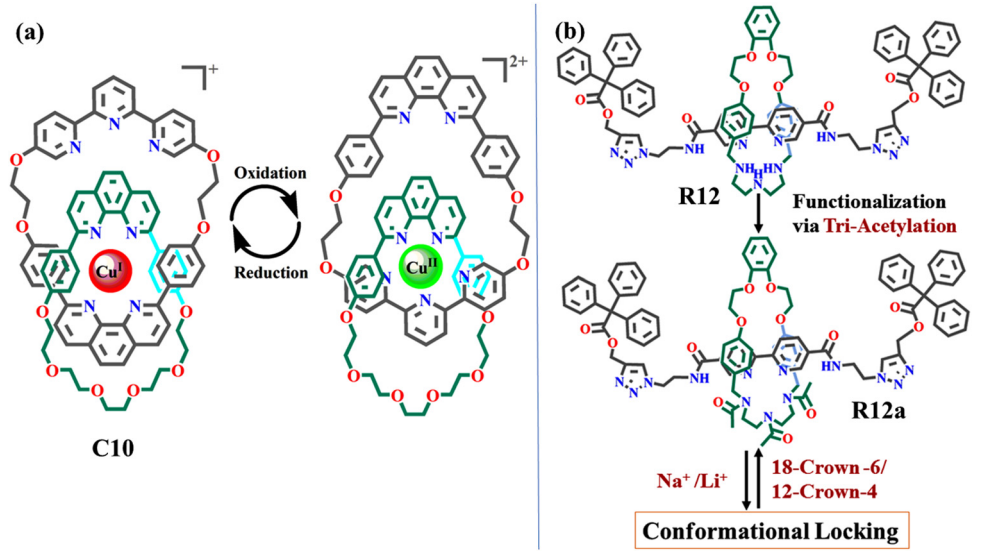

Fig. 9 (a) The electrochemically induced pirouetting motion of **C10**, (b) post-functionalization of **R12** and cation-induced conformational locking of **R12a**.

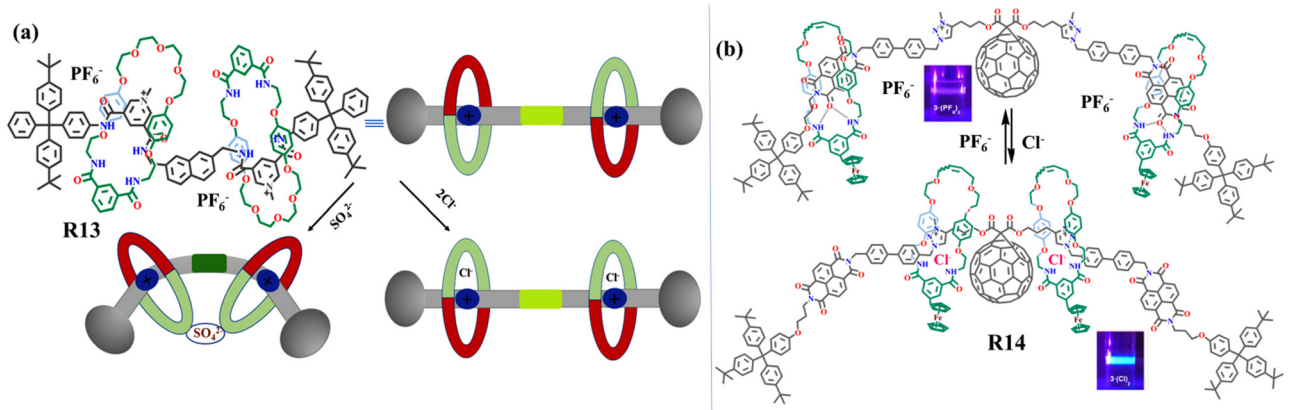

Fig. 10 The anion-induced dynamic properties in (a) **R13** and (b) **R14**.

time-resolved absorption, emission and electrochemical studies. The inset picture in Fig. 10b shows fluorescence ON/OFF switching, depending on the anion-induced wheel-axle interaction. A similar shuttling approach was also reported with other **W6** based rotaxanes.[73] Likewise, a heteroditopic [3]catenane (**C11**, Fig. 11a) was investigated that consists of a four-station centred macrocycle with two triazolium motifs and perylene diimide (PDI) units, mechanically bonded with two NO_2 group appended **W6** macrocycles. Circumrotatory motion of the NO_2-attached wheels around the larger wheel is triggered by Cl^-/PF_6^- and was further studied *via* NMR, UV-Vis and emission studies (Fig. 11a).[74]

Yuliang Li *et al.* with a similar heteroditopic **W6** wheel demonstrated a switchable [2]rotaxane (**R15**, Fig. 11b) containing triazole and ammonium stations.[47,68a] ^{1}H NMR studies showed that, upon protonation, the wheel switches to the ammonium station due to the HB interaction of the ammonium ion with the wheel-oxy ether cleft. The addition of base moves the wheel counterpart to the axle-triazolium station by destroying the HB. However, after the addition of Cl^-, the conformation of the wheel in **R15** is changed due to the co-operative interaction between the amide group of the isophthalamide wheel and the triazole CH proton of the axle (Fig. 11b).

In addition to the **W6** wheel, cation (Na^I and Ba^{II}) induced pirouetting motion in a heteroditopic **W7** macrocycle and pyridine *N*-oxide axle threaded rotaxane (**R16**, Fig. 12a) system was also demonstrated by Beer and co-workers. It was shown that the added cation interacts with the wheel-calix-ether and axle-*N*-oxide moieties. Removal of the cation moves the axle in the *N*-oxide direction to the isophthalamide cleft of the macrocycle due to HB interaction, which was analysed by NMR spectroscopy (Fig. 12a).[17b] Afterwards, Chiu and co-workers described Na^I-induced dynamicity in axle-amide threaded [2]rotaxane (**R17**, Fig. 12b), where Na^I ion shows the interaction between the wheel-ether and amide carbonyl cleft. Detachment

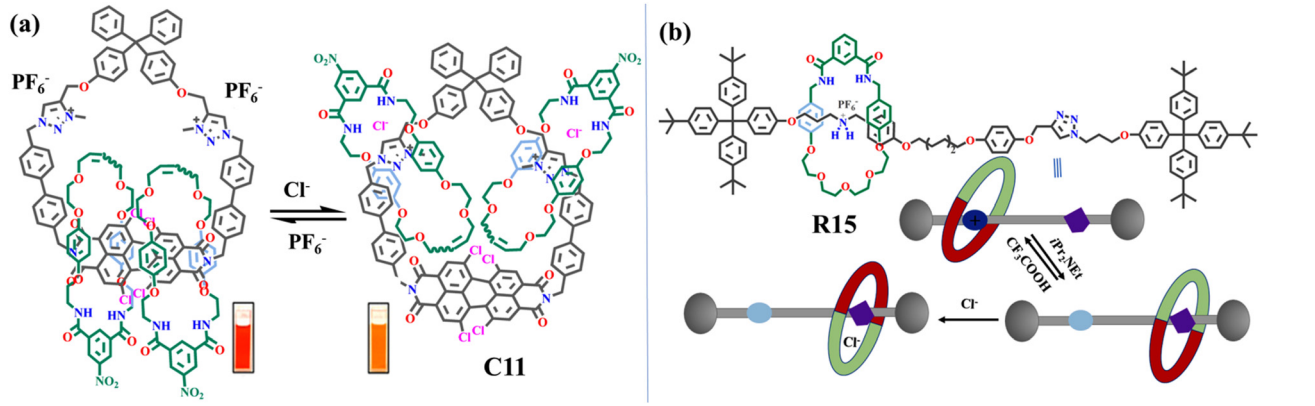

Fig. 11 Anion-induced fluorophoric shuttling in (a) **C11** and (b) **R15**. Inset pictures show the fluorescence colour changing upon positional change of wheel in **C11** and **R15**. (Adapted with copyright owner permission from ref. 73 and 74, Copyright 2018 and 2017, respectively, American Chemical Society.)

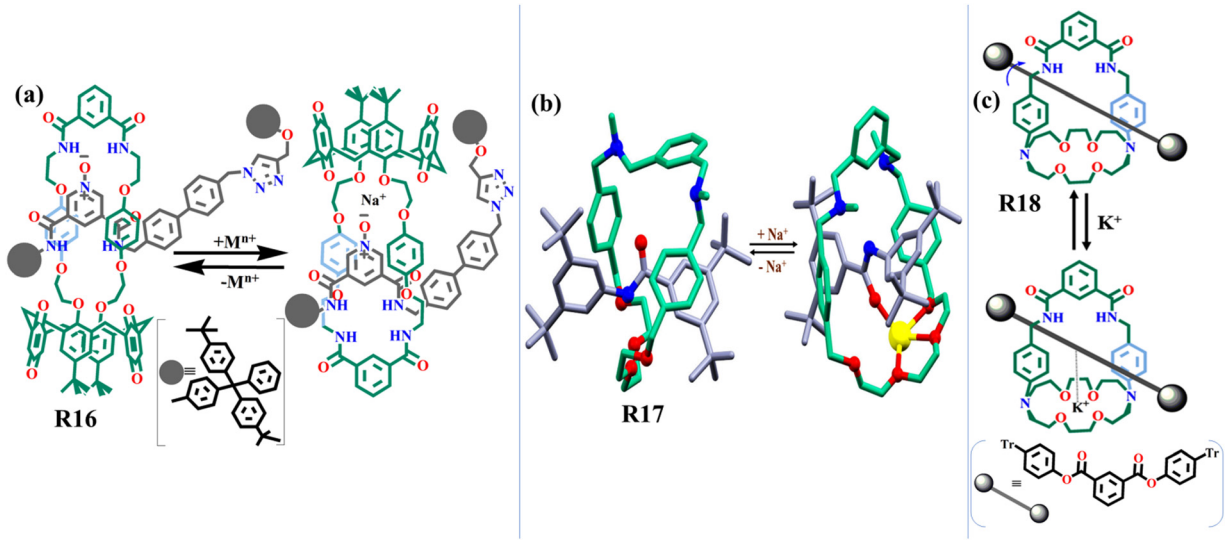

Fig. 12 Anion-induced shuttling in (a) **R16** and (b) **R17** (data from the Cambridge Crystallographic Data Centre (CCDC): **R17**: 1511677; Na bound **R17**: 1539017; and atoms are represented by blue for N, red for O and yellow for Na). (c) K^{I} based co-conformational locking of **R18**.

of Na^{I} induces motion within the wheel to get the oxy ether to bind with the axle-amide moiety (Fig. 12b).[18,75]

In a different approach, the Smith group demonstrated dynamic properties in a macrobicyclic **W10** wheel-based heteroditopic rotaxane host (**R18**, Fig. 12c). Here, K^{I} addition assists in co-conformational locking of **R18**, which was established by NMR spectroscopy (Fig. 12c).[19,43] Later, our group also investigated the dynamicity within a heteroditopic macrobicyclic **W11** wheel and pyridine-*N*-oxide axle threaded [2]pseudorotaxane (**P4**, Fig. 2). X-ray crystal analysis and ^{1}H NMR confirmed that the axle-pyridine-*N*-oxide dipole in **P4** is able to attain two different orientations in the corresponding neutral and tri-protonated states of the wheel.

In the tri-protonated state, the *N*-oxide dipole moves its position from the amide cleft and interacts with the protonated amine *via* HB interaction.[20]

Chen *et al.* reported a novel triply interlocked heteroditopic [2](3)catenane composed of a pyrazine-extended triptycene-derived tris(oxy-ether) wheel threaded by three *N*-methyltriazolium and dibenzyl ammonium cyclic ligands *via* HB templation.[76] Acid–base triggering causes stepwise molecular motion in the catenane, which generates four relatively stable co-conformations that were directly identified by NMR titration experiments.

Thus, exploration of such versatile dynamic behaviour within heteroditopic MIMs may be directed towards the construction of molecular machineries, molecular rachets, molecular ladders, *etc.*

4.3. Recognition and sensing

Over the last few years, huge interest has grown towards the utilization of rotaxanes and catenanes for the recognition and

sensing of a guest molecule in the cavity of host interlocked molecules. In general, a complementary size and preorganization of the three-dimensional cavity of the host molecules are the criteria for designing ideal sensor candidates. Prior to the sensing, the receptor MIMs are methodically equipped with fluorophoric and redox-active signalling groups for distinguishing among the incoming potential guests. Additionally, successful recognition offers a way to regulate the co-conformation of interlocked components' relative positions during molecular shuttling and switching. Accordingly, several approaches have been studied with the MIMs by different groups towards sensing and recognition of anions,[77] cations[78] or ion pairs.[10,79] In this section, specifically, heteroditopic MIMs-based recognition and sensing applications are described and divided into three major categories: (i) anion, (ii) cation and (iii) ion pair recognition/sensing.

4.3.1. Anion recognition and sensing. Anion recognition by the molecular receptor is becoming one of the key challenges in the supramolecular field. This is due to their weaker coordination arrangement, low charge densities, higher hydration energies and dependency on pH. The following examples of anion-bound heteroditopic MIMs are mainly directed by non-covalent interactions like HB, XB and mixed HB-XB interactions.

In 1998, the first interlocked catenated receptor for an anion was strategically designed by Sessler and Vögtle, with a bipyrrole amide group containing a monotopic macrocycle.[80] Later, Beer and co-workers widely explored this anion recognition area by specifically utilizing heteroditopic **W6** and imidazolium/pyridinium-amide containing axles that permit the formation of anion-driven threaded assemblies *via* HB interaction (**R19**, Fig. 13a). In this rotaxane (**R19**), upon Cl^- binding with the amide cleft of the wheel, a cathodic shifting occurred due to its readily accessible ferrocene/ferrocenium (Fc/Fc^+) redox couple (Fig. 13a).[81] In addition, a lanthanide (Ln^{III}) functionalized **W6** based type of Beer's rotaxane (**R20**, Fig. 13b), derived by utilizing unusual NO_3^- templation, leads to the sensing of F^-. By displacing a water molecule, F^- is directly coordinated with the Ln^{III} centre of the MIM and, thus, a sharp emission quenching is shown by the Ln^{III} centre (Fig. 13b).[82]

In 2014, XB based anion recognition was first demonstrated by Beer and group, and the XB donor MIMs resulted in better anion recognition compared to HB donors. It was shown that the pyridine associated **W6** wheel and bis-triazole pyridinium axle containing [2]rotaxane **R21** (Fig. 14a) host can selectively bind halide ion. Importantly, **R21** can recognise I^- in water through XB interaction, where the solubility in water is governed by permethylated β-cyclodextrin connected stoppers (Fig. 14a).[83] Further, this aqueous mediated anion sensing was advanced to photoactive anion sensing *via* altering the macrocyclic pyridinium component with a luminescent bipyridyl-$[Ru(bipy)_2]^{2+}$ motif that, upon sensing I^-, causes a metal to ligand charge transfer emission increment.[84] Another heteroditopic **W6** wheel-based Cl^- templated XB donor chiral [3]rotaxane (**R22**, Fig. 14b) was also described by Beer's group. Here, the chiral (*S*)-BINOL group in the axle moiety facilitates the optical sensing of dicarboxylate anion with emission quenching properties *via* combined HB–XB interactions and leads to the formation of 1 : 1 stoichiometric sandwich complexes (Fig. 14b).[85]

Additionally, indolocarbazole-oxy ether-based heteroditopic homo[2]catenane (**C12**, Fig. 15a) was reported by Jeong and group, directed towards Cl^- sensing over other competitive oxo-anions through the interaction between the bis-indolocarbazole motifs of the wheel and axle. Thus, Cl^- sensing causes the enhancement of the fluorescence intensity of the embedded indolocarbazole motif within the catenane (Fig. 15a).[86] Gunnlaugsson and co-workers followed another approach to synthesize a heteroditopic homo [2]catenane (**C13**, Fig. 15b) host which was studied towards PO_4^{3-} sensing over other anions through bis-triazolyl HB interactions (Fig. 15b).[87]

Thereafter, our group also described heteroditopic **W5** macrocycle directed anion binding studies of different MIM hosts, based on electrochemical, colorimetry and fluorescent responses. In this regard, active metal templated heteroditopic rotaxane was explored for the recognition of tetra butyl ammonium (TBA) anions by the axle-amide station *via* electrochemical and NMR titration studies.[45] During electrochemical titration, measurable anodic shifting of irreversible reduction waves of the phen motif and, during NMR titration, proton resonance shifting of the axle-amide indicate the recognition of $H_2PO_4^-$ over other anions. Colorimetric and fluorescent responding anion sensing was demonstrated by **W5** wheel

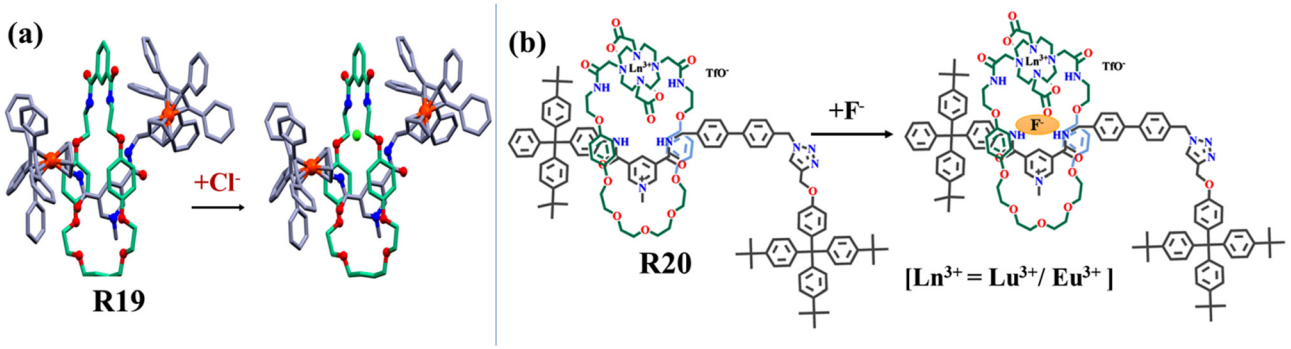

Fig. 13 (a) The electrochemical anion sensing of **R19** (data from the Cambridge Crystallographic Data Centre (CCDC): **R19**: 829486; atoms represented by blue for N, red for O and green for Cl), (b) lanthanide derived anion sensing of **R20**.

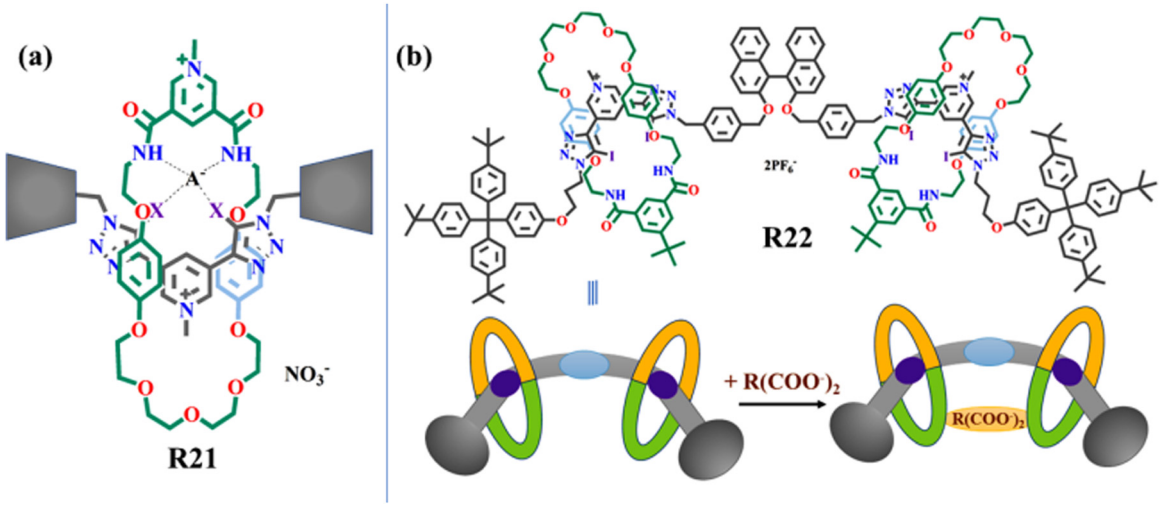

Fig. 14 (a) The cyclodextrin derived I^- sensing of **R21** in water. (b) The chiral *S*-binol derived dicarboxylate sensing of **R22**.

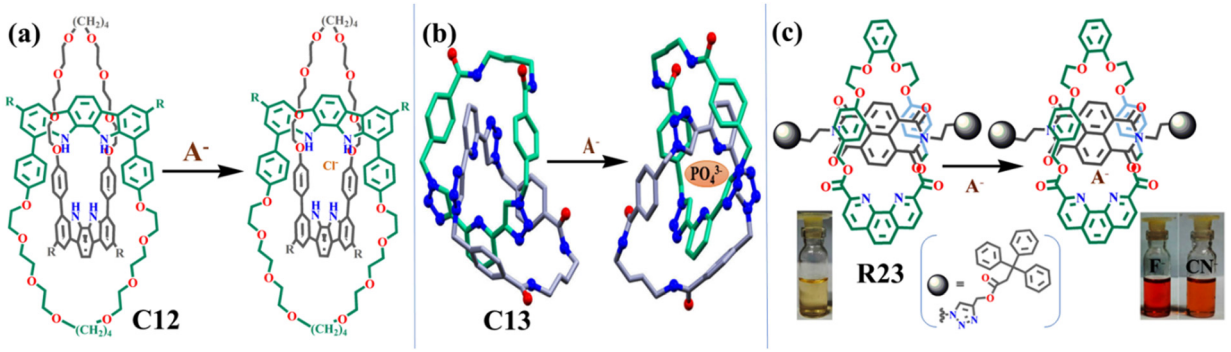

Fig. 15 (a) The indolocarbazole derived Cl^- sensing of **C12**. (b) The phosphate sensing of **C13** (data from the Cambridge Crystallographic Data Centre (CCDC): phosphate bound **C13**: 1469501; atoms are represented by blue for N and red for O). (c) The colorimetric anion sensing of **R23**. Inset pictures show the colorimetric sensing of F^- and CN^- by **R23**. (Adapted with copyright owner permission from ref. 55. Copyright 2022, Royal Society of Chemistry.)

and fluorophoric NDI axle containing [2]catenane (**C4**, Fig. 5) and [2]rotaxane (**R23**, Fig. 15c) hosts.[55] Here, both the MIMs served as the F^- and CN^- sensors (Fig. 15c) over other TBA anions *via* instantaneous changing of visual colours, which was further verified by UV-Vis-NIR, fluorescence titration, EPR and CV studies.

Here overall anion sensing studies of heteroditopic MIMs were elaborated and now significant cation sensing studies will be discussed in next subsection.

4.3.2. Cation sensing and recognition. Heteroditopic wheel-based cation sensing is scarce in literature as compared to that of anions. In this regard, recently our group investigated competitive cation sensing studies of the heteroditopic **W4** wheel and naphthyl group containing fluorophoric rotaxane **R24** and pyrene functionalized **R24a** (Fig. 16a) hosts. Upon addition of various alkali and transition metal ions, **R24** shows a slight perturbation in emission intensity for Zn^{II} and Cd^{II}. However, after post-functionalization of the tri-amine in **R24** with pyrene moieties, **R24a** shows higher emission intensity from the pyrene centre selectively for Zn^{II}, even in the presence of other competitive cations by a PET process that was verified by emission and UV-Vis titration studies (Fig. 16a).[88] In addition, another fluorophoric rotaxane (**R4**, Fig. 4) was studied with the same wheel and aryl vinyl motif containing axle towards cation sensing. In this rotaxane, the extended conjugation of the aryl vinyl moiety served as the signalling unit to sense Zn^{II} over another competitive alkali, alkaline and transition metal ions.[44c]

Afterwards, Leung and co-workers reported an amino axle threaded heteroditopic pyridinium-imine-oxy-ether wheel based fluorophoric [2]rotaxane (**R25**, Fig. 16b). **R25** shows direct sensing of Au^{III} over different alkali and transition metal ions by causing protonation of the axle-amine and termination of the PET process by turning on the fluorescence (Fig. 16b).[50,89]

4.3.3. Ion pair recognition. Co-operative ion pair binding by heteroditopic interlocked molecules is a rapidly developing field of interest. In this regard, Beer's group first reported a **W7** wheel-based alkali metal halide ion-pair recognition system

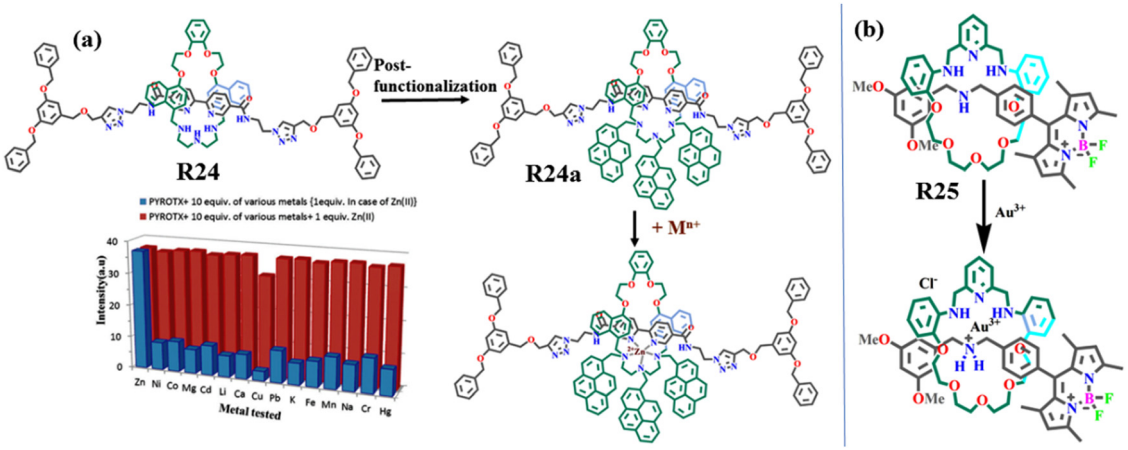

Fig. 16 (a) Fluorophoric Zn^{2+} sensing of **R24**. Inset pictures show selective sensing of Zn^{II} by **R24a**. (Adapted with copyright owner permission from ref. 88. Copyright 2021 Royal Society of Chemistry.) (b) Fluorophoric Au^{3+} sensing of **R25**.

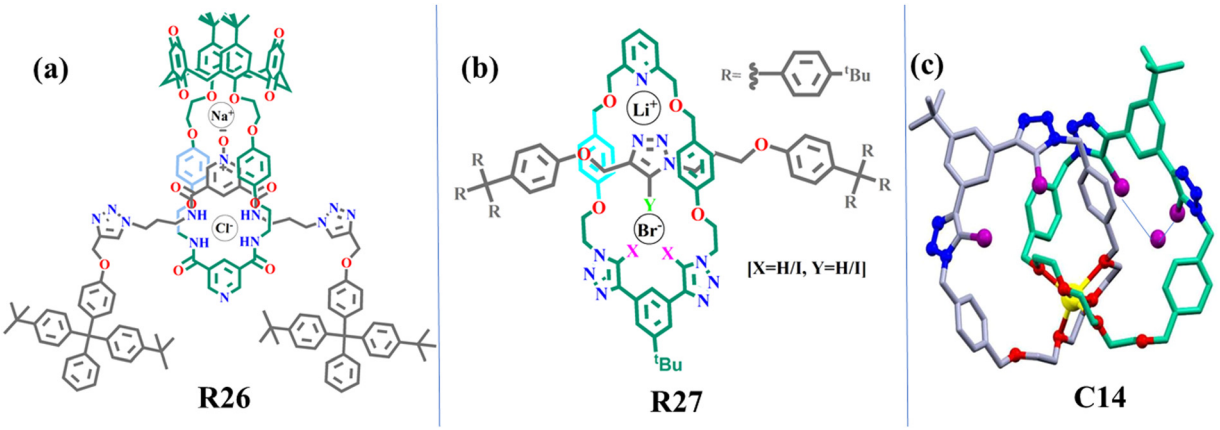

Fig. 17 The ion pair recognition of (a) **R26**, (b) **R27** and (c) **C14** (data from the Cambridge Crystallographic Data Centre (CCDC)): I^- bound **C14**: 2211718; atoms are represented by blue for N, red for O, yellow for Na and violet for [I].

R26 (Fig. 17a). Within the **R26** cavity, the cation is bound between the wheel-calixarene and axle-pyridine *N*-oxide moieties, whereas the anion interacts with the bis-amide cleft of the wheel and axle. Here, as found from the NMR titration experiments, co-bound Cl^- and Br^- of corresponding counter cations (Na^I and K^I) display greater binding affinity compared to I^- due to significant preorganisation of the **R26** host and a high cooperativity factor (Fig. 17a).[46b] Likewise, a transition metal-halide ion-pair rotaxane system was also designed with **W2** type wheel-based rotaxane, which, in the presence of Zn^{II} co-bound cation, shows the capability to bind Br^- and I^- anions cooperatively in a more competitive aqueous organic co-solvent mixture.[90]

Furthermore, lithium-halide ion pair recognition was recently established by an aza-crown containing **W9** wheel and XB axle-triazole threaded heteroditopic rotaxane (**R27**, Fig. 17b) by Beer and group. The co-bound Li^I ion assists in co-operative binding of Br^- over I^- in the XB macrocyclic triazole pocket (Fig. 17b).[91] Thereafter, a Na^I templated **W9**-based heteroditopic homo[2]catenane (**C14**, Fig. 17c) for ion–pair recognition was published in which a co-bound alkali metal atom (Na^I or K^I) in the oxy ether cage assists in the enhanced binding of Br^- and I^- within the triazolium halogen binding pocket (Fig. 17c).[17c,57b] Significantly, these recognition/sensing properties of MIMs may be extensively applied in extracting toxic ions in wastewater treatment, industrial purposes and other real life applications.

5. Summary and outlook

In this feature article, we addressed in detail different heteroditopic wheels composed of several multi-functional groups. We also thoroughly described the construction of a number of [*n*]pseudorotaxanes, rotaxanes and catenanes that are synthesized using such wheels. The heteroditopicity of these systems provides versatile aspects that can be applied in various directions of the molecular sciences. Thus, we have systematically

highlighted the significant functionalities of such MIMs in switching, shuttling, recognition and sensing, resulting from their mechanically bonded structures. The heteroditopicity of the systems is highlighted more precisely.

We envisage that our broad and detailed discussion on the new generation of heteroditopic wheel-based MIMs will add a new facet to the research of MIMs to clearly bring out significant properties. Although heteroditopic wheel based MIMs have been well described in this review article, there are still ample opportunities to be explored by integrating heteroditopicity in the construction of pseudorotaxanes, rotaxanes and catenanes. Such opportunities include (i) the incorporation of asymmetric functionalities within the supramolecular systems to assist in developing chiral interlocked molecules, chiral catalysis, *etc.*; (ii) the addition of an amide cleft, long alkyl chains and proper hydrophobic and hydrophilic moieties to trigger self-assembling properties to produce supramolecular gels, amphiphilic molecules and drug delivery characteristics; (iii) the use of lanthanide bound MIMs to help construct fluorescent materials, lanthanide catalysts, MRI contrasting agents, and bioimaging assays; (iv) the utilization of heteroditopic MIMs in solid material surfaces such as metallopolymers, metal–organic frameworks, advanced nano materials, *etc.*; and (v) the further incorporation of suitable functionalities within MIMs to construct molecular machines and other smart materials which are the most emerging topic in chemistry. In conclusion, heteroditopicity in the formation of a new generation of interlocked molecules heralds a new dawn in supramolecular chemistry, whose rapid progress in the near future will create potential significant impacts on various scientific fields.

Conflicts of interest

There are no conflicts to declare.

Acknowledgements

P. Ghosh acknowledges the SERB for the J. C. Bose National Fellowship (JCB/2021/000032) for financial assistance. M. Nandi acknowledges DST, Inspire (IF150113) and IACS, Kolkata, S. Bej acknowledges Council of Scientific & Industrial Research (CSIR) New Delhi and IACS, Kolkata, T. Jana acknowledges Council of Scientific & Industrial Research (CSIR) New Delhi for financial support.

Notes and references

1 (*a*) A. R. Pease, J. O. Jeppesen, J. F. Stoddart, Y. Luo, C. P. Collier and J. R. Heath, *Acc. Chem. Res.*, 2001, **34**, 433–444; (*b*) J. M. Baumes, J. J. Gassensmith, J. Giblin, J.-J. Lee, A. G. White, W. J. Culligan, W. M. Leevy, M. Kuno and B. D. Smith, *Nat. Chem.*, 2010, **2**, 1025–1030; (*c*) J.-P. Sauvage, *Angew. Chem., Int. Ed.*, 2017, **56**, 11080–11093; (*d*) R. Barat, T. Legigan, I. Tranoy-Opalinski, B. Renoux, E. Peraudeau, J. Clarhaut, P. Poinot, A. E. Fernandes, V. Aucagne, D. A. Leigh and S. Papot, *Chem. Sci.*, 2015, **6**, 2608–2613; (*e*) G. J. E. Davidson, S. Sharma and S. J. Loeb, *Angew. Chem., Int. Ed.*, 2010, **49**, 4938–4942; (*f*) J. F. Stoddart, *Angew. Chem., Int. Ed.*, 2017, **56**, 11094–11125; (*g*) G. Gil-Ramirez, D. A. Leigh and A. J. Stephens, *Angew. Chem., Int. Ed.*, 2015, **54**, 6110–6150; (*h*) M. Xue, Y. Yang, X. Chi, X. Yan and F. Huang, *Chem. Rev.*, 2015, **115**, 7398–7501; (*i*) M. J. Langton and P. D. Beer, *Acc. Chem. Res.*, 2014, **47**, 1935–1949; (*j*) A. Saura-Sanmartin, A. Pastor, A. Martinez-Cuezva, G. Cutillas-Font, M. Alajarin and J. Berna, *Chem. Soc. Rev.*, 2022, **51**, 4949–4976; (*k*) V. Balzani, A. Credi and M. Venturi, *Chem. Soc. Rev.*, 2009, **38**, 1542–1550.

2 (*a*) K. D. Haenni and D. A. Leigh, *Chem. Soc. Rev.*, 2010, **39**, 1240–1251; (*b*) G. Barin, A. Coskun, M. M. G. Fouda and J. F. Stoddart, *ChemPlusChem*, 2012, **77**, 159–185; (*c*) A. K. Mandal, M. Gangopadhyay and A. Das, *Chem. Soc. Rev.*, 2015, **44**, 663–676.

3 (*a*) B. Taghavi Shahraki, S. Maghsoudi, Y. Fatahi, N. Rabiee, S. Bahadorikhalili, R. Dinarvand, M. Bagherzadeh and F. Verpoort, *Coord. Chem. Rev.*, 2020, **423**, 213484; (*b*) A. Caballero, F. Zapata, N. G. White, P. J. Costa, V. Felix and P. D. Beer, *Angew. Chem., Int. Ed.*, 2012, **51**, 1876; (*c*) L. Liu, Y. Liu, P. Liu, J. Wu, Y. Guan, X. Hu, C. Lin, Y. Yang, X. Sun, J. Ma and L. Wang, *Chem. Sci.*, 2013, **4**, 1701–1706.

4 K. Yang, S. Chao, F. Zhang, Y. Pei and Z. Pei, *Chem. Commun.*, 2019, **55**, 13198–13210.

5 (*a*) H. Masai, Y. Oka and J. Terao, *Chem. Commun.*, 2022, **58**, 1644–1660; (*b*) Y. Akae, Y. Koyama, S. Kuwata and T. Takata, *Chem. – Eur. J.*, 2014, **20**, 17132–17136.

6 G. Cera, A. Arduini, A. Secchi, A. Credi and S. Silvi, *Chem. Rec.*, 2021, **21**, 1161–1181.

7 (*a*) A. K. Mandal, M. Suresh and A. Das, *Org. Biomol. Chem.*, 2011, **9**, 4811–4817; (*b*) N. Pearce, M. Tarnowska, N. J. Andersen, A. Wahrhaftig-Lewis, B. S. Pilgrim and N. R. Champness, *Chem. Sci.*, 2022, **13**, 3915–3941.

8 K. Kim, *Chem. Soc. Rev.*, 2002, **31**, 96–107.

9 (*a*) A. W. Heard and S. M. Goldup, *ACS Cent. Sci.*, 2020, **6**, 117–128; (*b*) J. Riebe and J. Niemeyer, *Eur. J. Org. Chem.*, 2021, 5106–5116.

10 S. J. Nicholson, S. R. Barlow and N. H. Evans, *Chemistry*, 2023, **5**, 106–118.

11 H.-Y. Zhou, Y. Han and C.-F. Chen, *Mater. Chem. Front.*, 2020, **4**, 12–28.

12 (*a*) M. S. Vickers and P. D. Beer, *Chem. Soc. Rev.*, 2007, **36**, 211–225; (*b*) K. M. Mullen and M. J. Gunter, *J. Org. Chem.*, 2008, **73**, 3336–3350.

13 A. Coskun, M. Hmadeh, G. Barin, F. Gandara, Q. Li, E. Choi, N. L. Strutt, D. B. Cordes, A. M. Z. Slawin, J. F. Stoddart, J.-P. Sauvage and O. M. Yaghi, *Angew. Chem., Int. Ed.*, 2012, **51**, 2160.

14 S. Saha, I. Ravikumar and P. Ghosh, *Chem. Commun.*, 2011, **47**, 6272–6274.

15 (*a*) S. Santra, S. Mukherjee, S. Bej, S. Saha and P. Ghosh, *Dalton Trans.*, 2015, **44**, 15198–15211; (*b*) S. Bej and P. Ghosh, *Dalton Trans.*, 2018, **47**, 13408–13418.

16 M. Nandi, S. Bej, T. K. Ghosh and P. Ghosh, *Chem. Commun.*, 2019, **55**, 3085–3088.

17 (*a*) D. A. Leigh and A. R. Thomson, *Org. Lett.*, 2006, **8**, 5377–5379; (*b*) L. M. Hancock and P. D. Beer, *Chem. Commun.*, 2011, **47**, 6012–6014; (*c*) H. M. Tay, Y. C. Tse, A. Docker, C. Gateley, A. L. Thompson, H. Kuhn, Z. Zhang and P. D. Beer, *Angew. Chem., Int. Ed.*, 2023, **62**, e202214785.

18 Y.-J. Lee, K.-S. Liu, C.-C. Lai, Y.-H. Liu, S.-M. Peng, R. P. Cheng and S.-H. Chiu, *Chem. – Eur. J.*, 2017, **23**, 9756–9760.

19 J. M. Mahoney, R. Shukla, R. A. Marshall, A. M. Beatty, J. Zajicek and B. D. Smith, *J. Org. Chem.*, 2002, **67**, 1436–1440.

20 S. Saha, S. Santra and P. Ghosh, *Org. Lett.*, 2015, **17**, 1854–1857.

21 (*a*) E. Wasserman, *J. Am. Chem. Soc.*, 1960, **82**, 4433; (*b*) H. L. Frisch and E. Wasserman, *J. Am. Chem. Soc.*, 1961, **83**, 3789.

22 I. T. Harrison and S. Harrison, *J. Am. Chem. Soc.*, 1967, **89**, 5723.

23 C. O. Dietrich-Buchecker, J. P. Sauvage and J. M. Kern, *J. Am. Chem. Soc.*, 1984, **106**, 3043.

24 (*a*) N. Solladie, J.-C. Chambron and J.-P. Sauvage, *J. Am. Chem. Soc.*, 1999, **121**, 3684–3692; (*b*) J. E. Beves, B. A. Blight, C. J. Campbell, D. A. Leigh and R. T. McBurney, *Angew. Chem., Int. Ed.*, 2011, **50**, 9260–9327.

25 (*a*) S. Santra, S. Bej, M. Nandi, P. Mondal and P. Ghosh, *Dalton Trans.*, 2017, **46**, 13300–13313; (*b*) M. Nandi, S. Santra, B. Akhuli and P. Ghosh, *Dalton Trans.*, 2017, **46**, 7421–7433; (*c*) S. Saha, S. Santra and P. Ghosh, *Eur. J. Inorg. Chem.*, 2014, 2029–2037.

26 J. Hu, L. Chen, J. Shen, J. Luo, P. Deng, Y. Ren, H. Zeng, W. Feng and L. Yuan, *Chem. Commun.*, 2014, **50**, 8024–8027.

27 A. I. Prikhodko and J.-P. Sauvage, *J. Am. Chem. Soc.*, 2009, **131**, 6794–6807.
28 S. Saha, I. Ravikumar and P. Ghosh, *Chem. – Eur. J.*, 2011, **17**, 13712.
29 S. Bej, M. Nandi, T. K. Ghosh and P. Ghosh, *Dalton Trans.*, 2019, **48**, 6853–6862.
30 F. Durola, J.-P. Sauvage and O. S. Wenger, *Coord. Chem. Rev.*, 2010, **254**, 1748–1759.
31 C. Gong and H. W. Gibson, *Macromolecules*, 1996, **29**, 7029–7033.
32 D. A. Leigh, V. Marcos and M. R. Wilson, *ACS Catal.*, 2014, **4**, 4490–4497.
33 X. Ma and H. Tian, *Chem. Soc. Rev.*, 2010, **39**, 70–80.
34 P. D. Beer, M. R. Sambrook and D. Curiel, *Chem. Commun.*, 2006, 2105–2117.
35 B. D. Smith, *Beilstein J. Org. Chem.*, 2015, **11**, 2540–2548.
36 (*a*) A. Saura-Sanmartin and C. A. Schalley, *Chem*, 2023, **9**, 823–846; (*b*) H. V. Schroeder and C. A. Schalley, *Chem. Sci.*, 2019, **10**, 9626–9639.
37 J. E. M. Lewis, M. Galli and S. M. Goldup, *Chem. Commun.*, 2017, **53**, 298–312.
38 S. J. Loeb, *Chem. Soc. Rev.*, 2007, **36**, 226–235.
39 L. Chen, X. Sheng, G. Li and F. Huang, *Chem. Soc. Rev.*, 2022, **51**, 7046–7065.
40 (*a*) X.-Q. Wang, W.-J. Li, W. Wang and H.-B. Yang, *Chem. Commun.*, 2018, **54**, 13303–13318; (*b*) N. Hoyas Perez and J. E. M. Lewis, *Org. Biomol. Chem.*, 2020, **18**, 6757–6780; (*c*) N. H. Evans, *Eur. J. Org. Chem.*, 2019, 3320–3343; (*d*) D. R. Kohn, L. D. Movsisyan, A. L. Thompson and H. L. Anderson, *Org. Lett.*, 2017, **19**, 348–351.
41 (*a*) S. S. Zhu, P. J. Carroll and T. M. Swager, *J. Am. Chem. Soc.*, 1996, **118**, 8713–8714; (*b*) S. S. Zhu and T. M. Swager, *J. Am. Chem. Soc.*, 1997, **119**, 12568–12577.
42 (*a*) P. Mobian, J.-P. Collin and J.-P. Sauvage, *Tetrahedron Lett.*, 2006, **47**, 4907–4909; (*b*) F. Durola and J.-P. Sauvage, *Angew. Chem., Int. Ed.*, 2007, **46**, 3537–3540.
43 R. Shukla, M. J. Deetz and B. D. Smith, *Chem. Commun.*, 2000, 2397–2398.
44 (*a*) S. Saha, S. Santra, B. Akhuli and P. Ghosh, *J. Org. Chem.*, 2014, **79**, 11170–11178; (*b*) S. Santra and P. Ghosh, *Eur. J. Org. Chem.*, 2017, 1583–1593; (*c*) S. Bej, M. Nandi and P. Ghosh, *Org. Biomol. Chem.*, 2022, **20**, 7284–7293.
45 M. Nandi, S. Bej, S. Bhunia and P. Ghosh, *ChemElectroChem*, 2020, **7**, 1038–1047.
46 (*a*) T. Bunchuay, A. Docker, A. J. Martinez-Martinez and P. D. Beer, *Angew. Chem., Int. Ed.*, 2019, **58**, 13823–13827; (*b*) R. C. Knighton and P. D. Beer, *Chem. Commun.*, 2014, **50**, 1540–1542; (*c*) N. H. Evans, C. J. Serpell and P. D. Beer, *Chem. Commun.*, 2011, **47**, 8775–8777.
47 H. Zheng, W. Zhou, J. Lv, X. Yin, Y. Li, H. Liu and Y. Li, *Chem. – Eur. J.*, 2009, **15**, 13253.
48 G. De, Bo, G. Dolphijn, C. T. McTernan and D. A. Leigh, *J. Am. Chem. Soc.*, 2017, **139**, 8455–8457.
49 (*a*) Y.-W. Wu, P.-N. Chen, C.-F. Chang, C.-C. Lai and S.-H. Chiu, *Org. Lett.*, 2015, **17**, 2158–2161; (*b*) C.-Y. Tsai, C.-C. Lai, Y.-H. Liu, S.-M. Peng, R. P. Cheng and S.-H. Chiu, *J. Org. Chem.*, 2018, **83**, 5619–5628.
50 S.-M. Chan, F.-K. Tang, C.-S. Kwan, C.-Y. Lam, S. C. K. Hau and K. C.-F. Leung, *Mater. Chem. Front.*, 2019, **3**, 2388–2396.
51 J. P. Sauvage and J. Weiss, *J. Am. Chem. Soc.*, 1985, **107**, 6108.
52 (*a*) J. Guilhem, C. Pascard, J. P. Sauvage and J. Weiss, *J. Am. Chem. Soc.*, 1988, **110**, 8711; (*b*) F. Bitsch, C. O. Dietrich-Buchecker, A. K. Khemiss, J. P. Sauvage and A. Van Dorsselaer, *J. Am. Chem. Soc.*, 1991, **113**, 4023.
53 D. B. Amabilino, C. O. Dietrich-Buchecker, A. Livoreil, L. Perez-Garcia, J.-P. Sauvage and J. F. Stoddart, *J. Am. Chem. Soc.*, 1996, **118**, 3905.
54 (*a*) J. D. Megiatto, Jr. and D. I. Schuster, *J. Am. Chem. Soc.*, 2008, **130**, 12872–12873; (*b*) J. D. Megiatto, Jr. and D. I. Schuster, *Chem. – Eur. J.*, 2009, **15**, 5444.
55 M. Nandi, S. Bej and P. Ghosh, *Dalton Trans.*, 2022, **51**, 13507–13514.
56 N. H. Evans, C. J. Serpell and P. D. Beer, *Chem. – Eur. J.*, 2011, **17**, 7734.
57 (*a*) A. V. Leontiev, C. J. Serpell, N. G. White and P. D. Beer, *Chem. Sci.*, 2011, **2**, 922–927; (*b*) R. C. Knighton and P. D. Beer, *Org. Chem. Front.*, 2021, **8**, 2468–2472.
58 J. E. M. Lewis, *Org. Biomol. Chem.*, 2019, **17**, 2442–2447.
59 (*a*) S.-T. Tung, C.-C. Lai, Y.-H. Liu, S.-M. Peng and S.-H. Chiu, *Angew. Chem., Int. Ed.*, 2013, **52**, 13269–13272; (*b*) A. Inthasot, S.-T. Tung and S.-H. Chiu, *Acc. Chem. Res.*, 2018, **51**, 1324–1337.
60 Y. Nakatani, Y. Furusho and E. Yashima, *Angew. Chem., Int. Ed.*, 2010, **49**, 5463.
61 (*a*) C. Lincheneau, B. Jean-Denis and T. Gunnlaugsson, *Chem. Commun.*, 2014, **50**, 2857–2860; (*b*) A. F. Henwood, I. N. Hegarty, E. P. McCarney, J. I. Lovitt, S. Donohoe and T. Gunnlaugsson, *Coord. Chem. Rev.*, 2021, **449**, 214206.
62 A. Credi, S. Dumas, S. Silvi, M. Venturi, A. Arduini, A. Pochini and A. Secchi, *J. Org. Chem.*, 2004, **69**, 5881–5887.
63 C. R. Benson, A. I. Share, M. G. Marzo and A. H. Flood, *Inorg. Chem.*, 2016, **55**, 3767–3776.
64 M. Chen, S. Han, L. Jiang, S. Zhou, F. Jiang, Z. Xu, J. Liang and S. Zhang, *Chem. Commun.*, 2010, **46**, 3932–3934.
65 (*a*) W. Zhou, J. Li, X. He, C. Li, J. Lv, Y. Li, S. Wang, H. Liu and D. Zhu, *Chem. – Eur. J.*, 2008, **14**, 754–763; (*b*) Y. Zhao, Y. Li, S.-W. Lai, J. Yang, C. Liu, H. Liu, C.-M. Che and Y. Li, *Org. Biomol. Chem.*, 2011, **9**, 7500–7503.
66 M. J. Barrell, D. A. Leigh, P. J. Lusby and A. M. Z. Slawin, *Angew. Chem., Int. Ed.*, 2008, **47**, 8036–8039.
67 X. Li, J. Y. C. Lim and P. D. Beer, *Chem. – Eur. J.*, 2018, **24**, 17788–17795.
68 (*a*) W. Yang, Y. Li, H. Liu, L. Chi and Y. Li, *Small*, 2012, **8**, 504–516; (*b*) S. Erbas-Cakmak, D. A. Leigh, C. T. McTernan and A. L. Nussbaumer, *Chem. Rev.*, 2015, **115**, 10081–10206; (*c*) R. Benny, D. Sahoo, A. George and S. De, *ChemistryOpen*, 2022, **11**, e202200128.
69 M. C. Jimenez, C. Dietrich-Buchecker and J.-P. Sauvage, *Angew. Chem., Int. Ed.*, 2000, **39**, 3284–3287.
70 M. C. Jimenez-Molero, C. Dietrich-Buchecker and J.-P. Sauvage, *Chem. – Eur. J.*, 2002, **8**, 1456–1466.
71 S. Santra and P. Ghosh, *New J. Chem.*, 2020, **44**, 5947–5964.
72 M. J. Langton and P. D. Beer, *Chem. – Eur. J.*, 2012, **18**, 14406.
73 T. A. Barendt, I. Rasovic, M. A. Lebedeva, G. A. Farrow, A. Auty, D. Chekulaev, I. V. Sazanovich, J. A. Weinstein, K. Porfyrakis and P. D. Beer, *J. Am. Chem. Soc.*, 2018, **140**, 1924–1936.
74 T. A. Barendt, L. Ferreira, I. Marques, V. Felix and P. D. Beer, *J. Am. Chem. Soc.*, 2017, **139**, 9026–9037.
75 S.-Y. Hsueh, C.-T. Kuo, T.-W. Lu, C.-C. Lai, Y.-H. Liu, H.-F. Hsu, S.-M. Peng, C.-H. Chen and S.-H. Chiu, *Angew. Chem., Int. Ed.*, 2010, **49**, 9170.
76 Z. Meng, Y. Han, L.-N. Wang, J.-F. Xiang, S.-G. He and C.-F. Chen, *J. Am. Chem. Soc.*, 2015, **137**, 9739–9745.
77 M. V. R. Raju and H.-C. Lin, *Org. Lett.*, 2013, **15**, 1274–1277.
78 M. Denis, J. Pancholi, K. Jobe, M. Watkinson and S. M. Goldup, *Angew. Chem., Int. Ed.*, 2018, **57**, 5310–5314.
79 J. R. Romero, G. Aragay and P. Ballester, *Chem. Sci.*, 2017, **8**, 491–498.
80 A. Andrievsky, F. Ahuis, J. L. Sessler, F. Voegtle, D. Gudat and M. Moini, *J. Am. Chem. Soc.*, 1998, **120**, 9712–9713.
81 N. H. Evans, C. J. Serpell, N. G. White and P. D. Beer, *Chem. – Eur. J.*, 2011, **17**, 12347.
82 M. J. Langton, O. A. Blackburn, T. Lang, S. Faulkner and P. D. Beer, *Angew. Chem., Int. Ed.*, 2014, **53**, 11463–11466.
83 M. J. Langton, S. W. Robinson, I. Marques, V. Felix and P. D. Beer, *Nat. Chem.*, 2014, **6**, 1039–1043.
84 M. J. Langton, I. Marques, S. W. Robinson, V. Felix and P. D. Beer, *Chem. – Eur. J.*, 2016, **22**, 185–192.
85 J. Y. C. Lim, I. Marques, V. Felix and P. D. Beer, *Angew. Chem., Int. Ed.*, 2018, **57**, 584–588.
86 M. K. Chae, J.-M. Suk and K.-S. Jeong, *Tetrahedron Lett.*, 2010, **51**, 4240–4242.
87 J. P. Byrne, S. Blasco, A. B. Aletti, G. Hessman and T. Gunnlaugsson, *Angew. Chem., Int. Ed.*, 2016, **55**, 8938–8943.
88 S. Bej, M. Nandi and P. Ghosh, *Dalton Trans.*, 2021, **50**, 294–303.
89 K. M. Bak, K. Porfyrakis, J. J. Davis and P. D. Beer, *Mater. Chem. Front.*, 2020, **4**, 1052–1073.
90 A. Brown, K. M. Mennie, O. Mason, N. G. White and P. D. Beer, *Dalton Trans.*, 2017, **46**, 13376–13385.
91 V. K. Munasinghe, J. Pancholi, D. Manawadu, Z. Zhang and P. D. Beer, *Chem. – Eur. J.*, 2022, **28**, e202201209.

